

A reliable, sensitive and fast optical fiber hydrogen sensor based on surface plasmon resonance

Cédric Perrotton,¹ Ruud. J. Westerwaal,² Nicolas Javahiraly,¹ Martin Slaman,² Herman Schreuders,² Bernard Dam,^{2,*} and Patrick Meyrueis¹

¹ Laboratoire des Systèmes Photoniques- Institut d'Électronique du Solide et des Systèmes, Université de Strasbourg, Pole API, Bvd Sébastien Brant, 67400 Illkirch, France

² Department of Chemical Engineering, MECS, Delft University of Technology Julianalaan136, 2628 BL Delft, The Netherlands

*B.dam@tudelft.nl

Abstract: We report for the first time on the experimental response of a Surface Plasmon Resonance fiber optic sensor based on wavelength modulation for hydrogen sensing. This approach of measuring the hydrogen concentration makes the sensor insensitive to intensity fluctuations. The intrinsic fiber sensor developed provides remote sensing and enables the possibility of multi-points sensing. The sensor consists of a multilayer of 35 nm Au / 180 nm SiO₂/ Pd deposited on a step- index multimode fiber core. The sensitivity and selectivity of the sensor are optimal at a Pd thickness of 3.75 nm. The sensor is sensitive to a hydrogen concentration ranging between 0.5 and 4% H₂ in Ar, with a response time less than 15 s.

©2013 Optical Society of America

OCIS codes: (280.0280) Remote sensing and sensors; (060.2370) Fiber optics sensors; (240.6680) Surface plasmons.

References and links

1. J. Villatoro and D. Monzón-Hernández, "Fast detection of hydrogen with nano fiber tapers coated with ultra thin palladium layers," *Opt. Express* **13**(13), 5087–5092 (2005).
2. D. Luna-Moreno, D. Monzon-Hernandez, S. Calixto-Carrera, and R. Espinosa-Luna, "Tailored Pd-Au layer produced by conventional evaporation process for hydrogen sensing," *Opt. Lasers Eng.* **49**(6), 693–697 (2011).
3. A. Trouillet, E. Marin, and C. Veillas, "Fibre gratings for hydrogen sensing," *Meas. Sci. Technol.* **17**(5), 1124–1128 (2006).
4. B. Sutapun, M. Tabib-Azar, and A. Kazemi, "Pd-coated elastooptic fiber optic Bragg grating sensors for multiplexed hydrogen sensing," *Sens. Actuators B* **60**(1), 27–34 (1999).
5. M. Buric, K. P. Chen, M. Bhattarai, P. R. Swinehart, and M. Maklad, "Active fiber Bragg grating hydrogen sensors for all-temperature operation," *IEEE Photon. Technol. Lett.* **19**(5), 255–257 (2007).
6. R. Maier, B. Jones, J. Barton, S. McCulloch, T. Allsop, J. Jones, and I. Bennion, "Fibre optics in palladium-based hydrogen sensing," *J. Opt. A, Pure Appl. Opt.* **9**(6), S45–S59 (2007).
7. X. Wei, T. Wei, H. Xiao, and Y. Lin, "Nano-structured Pd-long period fiber gratings integrated optical sensor for hydrogen detection," *Sens. Actuators B* **134**(2), 687–693 (2008).
8. K. Schroeder, W. Ecke, and R. Willsch, "Optical fiber Bragg grating hydrogen sensor based on evanescent-field interaction with palladium thin-film transducer," *Opt. Lasers Eng.* **47**(10), 1018–1022 (2009).
9. L. Boon-Brett, J. Bousek, G. Black, P. Moretto, P. Castello, T. Hübert, and U. Banach, "Identifying performance gaps in hydrogen safety sensor technology for automotive and stationary applications," *Int. J. Hydrogen Energy* **35**(1), 373–384 (2010).
10. B. Liedberg, C. Nylander, and I. Lunström, "Surface plasmon resonance for gas detection and biosensing," *Sens. Actuators* **4**, 299–304 (1983).
11. I. Garcés, C. Aldea, and J. Mateo, "Four-layer chemical fibre optic plasmon-based sensor," *Sens. Actuators B* **7**(1-3), 771–774 (1992).
12. C. Lavers and J. Wilkinson, "A waveguide-coupled surface-plasmon sensor for an aqueous environment," *Sens. Actuators B* **22**(1), 75–81 (1994).
13. B. Chadwick and M. Gal, "Enhanced optical detection of hydrogen using the excitation of surface plasmons in palladium," *Appl. Surf. Sci.* **68**(1), 135–138 (1993).
14. X. Bévenot, A. Trouillet, C. Veillas, H. Gagnaire, and M. Clement, "Surface plasmon resonance hydrogen sensor using an optical fibre," *Meas. Sci. Technol.* **13**(1), 118–124 (2002).

15. C. Perrotton, M. Slaman, N. Javahiraly, H. Schreuders, B. Dam, and P. Meyrueis, "Wavelength response of a surface plasmon resonance palladium-coated optical fiber sensor for hydrogen detection," *Opt. Eng.* **50**(1), 014403 (2011).
16. D. Nau, A. Seidel, R. B. Orzekowsky, S. H. Lee, S. Deb, and H. Giessen, "Hydrogen sensor based on metallic photonic crystal slabs," *Opt. Lett.* **35**(18), 3150–3152 (2010).
17. C. Langhammer, I. Zorić, B. Kasemo, and B. M. Clemens, "Hydrogen storage in Pd nanodisks characterized with a novel nanoplasmonic sensing scheme," *Nano Lett.* **7**(10), 3122–3127 (2007).
18. C. Langhammer, E. M. Larsson, B. Kasemo, and I. Zorić, "Indirect nanoplasmonic sensing: Ultrasensitive experimental platform for nanomaterials science and optical nanocalorimetry," *Nano Lett.* **10**(9), 3529–3538 (2010).
19. N. Liu, M. Mesch, T. Weiss, M. Hentschel, and H. Giessen, "Infrared perfect absorber and its application as plasmonic sensor," *Nano Lett.* **10**(7), 2342–2348 (2010).
20. E. Maeda, S. Mikuriya, K. Endo, I. Yamada, A. Suda, and J. J. Delaunay, "Optical hydrogen detection with periodic subwavelength palladium hole arrays," *Appl. Phys. Lett.* **95**(13), 133504 (2009).
21. N. R. Fong, P. Berini, and R. N. Tait, "Modeling and design of hydrogen gas sensors based on a membrane-supported surface plasmon waveguide," *Sens. Act. B*, 285–291 (2011).
22. R. Jorgenson and S. Yee, "A fiber-optic chemical sensor based on surface plasmon resonance," *Sens. Actuators B* **12**(3), 213–220 (1993).
23. C. Perrotton, N. Javahiraly, M. Slaman, B. Dam, and P. Meyrueis, "Fiber optic Surface Plasmon Resonance sensor based on wavelength modulation for hydrogen sensing," *Opt. Express* **19**(S6 Suppl 6), A1175–A1183 (2011).
24. K. von Rottkay, M. Rubin, and P. Duine, "Refractive index changes of Pd-coated magnesium lanthanide switchable mirrors upon hydrogen insertion," *J. Appl. Phys.* **85**(1), 408–413 (1999).
25. M. A. Ordal, L. L. Long, R. J. Bell, S. E. Bell, R. R. Bell, R. W. Alexander, Jr., and C. A. Ward, "Optical properties of the metals Al, Co, Cu, Au, Fe, Pb, Ni, Pd, Pt, Ag, Ti, and W in the infrared and far infrared," *Appl. Opt.* **22**(7), 1099–20 (1983).
26. I. Pockrand, "Resonance anomalies in the light intensity reflected at silver gratings with dielectric coatings," *J. Phys. D* **9**(17), 2423–2432 (1976).
27. R. Gremaud, M. Gonzalez-Silveira, Y. Pivak, S. de Man, M. Slaman, H. Schreuders, B. Dam, and R. Griessen, "Hydrogenography of PdHx thin films: Influence of H-induced stress relaxation processes," *Acta Mater.* **57**(4), 1209–1219 (2009).
28. Y. Pivak, R. Gremaud, K. Gross, M. Gonzalez-Silveira, A. Walton, D. Book, H. Schreuders, B. Dam, and R. Griessen, "Effect of the substrate on the thermodynamic properties of PdHx films studied by hydrogenography," *Scr. Mater.* **60**(5), 348–351 (2009).
29. F. A. Lewis, ed., *The Palladium Hydrogen System* (Academic Press, London and New York, 1967).
30. R. Gremaud, *Hydrogenography: A Thin Film Optical Combinatorial Study of Hydrogen Storage Materials* (Ipskamp, 2008).
31. X. Bévenot, A. Trouillet, C. Veillas, H. Gagnaire, and M. Clement, "Hydrogen leak detection using an optical fibre sensor for aerospace applications," *Sens. Actuators B* **67**(1-2), 57–67 (2000).
32. Z. Zhao, M. Carpenter, H. Xia, and D. Welch, "All-optical hydrogen sensor based on a high alloy content palladium thin film," *Sens. Actuators B* **113**(1), 532–538 (2006).
33. Z. Zhao, Y. Sevryugina, M. A. Carpenter, D. Welch, and H. Xia, "All-optical hydrogen-sensing materials based on tailored palladium alloy thin films," *Anal. Chem.* **76**(21), 6321–6326 (2004).
34. J. Huiberts, J. Rector, R. Wijngaarden, S. Jetten, D. De Groot, B. Dam, N. Koeman, R. Griessen, B. Hjorvarsson, S. Olafsson, and Y. S. Cho, "Synthesis of yttriumtrihydride films for ex-situ measurements," *J. Alloy. Comp.* **239**(2), 158–171 (1996).
35. B. Fisher and D. Malocha, "A study on the aging of ultra-thin Palladium films on SAW hydrogen gas sensors," in *IEEE Frequency Control Symposium*, pp. 242–247 (2010).
36. F. Favier, E. C. Walter, M. P. Zach, T. Benter, and R. M. Penner, "Hydrogen sensors and switches from electrodeposited palladium mesowire arrays," *Science* **293**(5538), 2227–2231 (2001).
37. K. Kalli, A. Othonos, and C. Christofides, "Characterization of reflectivity inversion, α - and β -phase transitions and nanostructure formation in hydrogen activated thin Pd films on silicon based substrates," *J. Appl. Phys.* **91**(6), 3829–3840 (2002).
38. A. Tittl, P. Mai, R. Taubert, D. Dregely, N. Liu, and H. Giessen, "Palladium-based plasmonic perfect absorber in the visible wavelength range and its application to hydrogen sensing," *Nano Lett.* **11**, 4366–4369 (2011).

1. Introduction

Hydrogen may be the future clean carrier of energy since fuel cells allow for a clean, CO₂ emission-free conversion into electrical power. However, the use of hydrogen as an energy carrier introduces safety challenges. Hydrogen is a flammable and highly explosive gas when mixed with oxygen. The flammability ranges from 4% up to 74.5% H₂ in air (here we refer to the volumetric percentage), with a minimal ignition energy of only 0.02 mJ. Moreover, hydrogen is prone to leak through seals and micro-cracks since hydrogen is the lightest and the smallest molecule. As hydrogen is undetectable by human senses, cheap reliable hydrogen sensors are urgently needed in order to use safely hydrogen.

Contrary to electrical sensors, optical fiber sensors are electrically isolated which makes them an excellent candidate for operating in explosive environments. There is no risk of gas ignition since the optical detector has no electrical contacts and does not generate sparks nor relies on heat exchanges. Numerous optical fiber hydrogen sensors have been previously developed, but none of them meet all the specifications recommended by industries or governmental agencies. In particular, their response times are often too slow. At present, fast optical fiber sensors are based on intensity modulation, and show a typical response time of 5–10 s at 4% H₂ in an inert gas environment (Ar, N₂) [1, 2]. However, for practical purposes, these sensors have the disadvantage that they need to be calibrated to compensate for irreproducible connection losses. In contrast, fiber sensors based on wavelength modulation are more reliable since they are insensitive to fluctuations of the light source. Nevertheless, the response time increases to more than 30 s, for optical fiber sensors based on wavelength modulation. This is due to the use of a thick (more than 30 nm) sensing material layer [3–8]. In spite of the fact that the diffusion is not the limiting step for nanometric films, thinner films show a faster response. Note that for most applications the response time of a hydrogen sensor is preferred to be less than 1–3 s [9].

In this paper we demonstrate that plasmonic sensor is a solution to obtain a fast and sensitive hydrogen fiber sensor based on wavelength modulation. We make use of the fact that Surface Plasmon Resonance (SPR) sensors in general show a high sensitivity even for very thin metal sensing layers for optimizing the response time. Numerous SPR sensors have been already developed for bio-sensing and gas applications since Liebborg and Nylander's work in 1982 [10]. The development of SPR sensors consists mainly of engineering the plasmonic multilayer transducer to tune the dispersion relation of Surface plasmon, and optimize the performance of the sensor for the application considered [11, 12]. Chadwick demonstrated the first time a SPR hydrogen sensor by using the SPR at the Pd air interface in the Kretschman's configuration [13]. The hydrogen absorption by the Pd film alters the propagation constant of the Surface Plasmon (SP). To improve the sensitivity of the SPR sensor and to be able to develop compact devices, new designs based on multimode fiber sensor [14, 15], nanostructured surface [16], Pd Localized SPR [17, 18], Nanoantenna [19], Extraordinary Transmission [20] or Mach Zehnder Interferometer (MZI) [21] have been proposed. Interestingly, SPR fiber sensors have certain advantages over other types of sensors such as remote sensing and the possibility of multi-points detection [22]. These sensors consisted of a Pd layer deposited on the core of the optical fiber after removing a part of the cladding [14, 15]. However, the Numerical Aperture of the optical fiber limits the coupling between the propagating light and the Surface Plasmon. In a previous work [23], we proposed on the basis of a computational analysis to deposit a multilayer stack made of Ag, SiO₂ and Pd in order to overcome the mismatch of the propagative constant between the guided modes and the SP propagating at the Pd air interface, and then satisfied the resonance condition. In this paper, we show the feasibility of such structure. In particular, we demonstrate a sensitive, fast and robust Surface Plasmon Resonance (SPR) hydrogen fiber sensor based on wavelength modulation.

2. The proposed model system

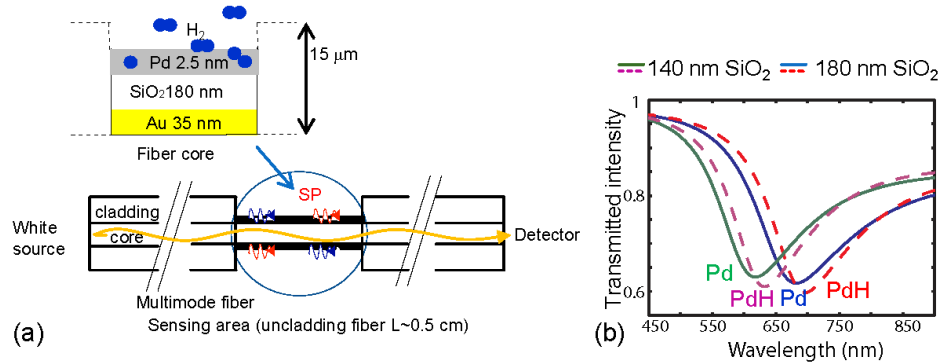


Fig. 1. (a) Schematic representation of the way the sensitive material is deposited on the fiber core, after removing the cladding. (b) The simulated transmitted intensity as a function of the wavelength for two different SiO_2 thicknesses. The line and the dashed line represent respectively the metallic and the hydrogenated states.

Our design consists of a multilayer of 35 nm Au / 180 nm SiO_2 / thin Pd layer deposited on a step-index multimode fiber core, as shown in Fig. 1(a). When the resonance condition of the Surface Plasmon (SP) is fulfilled, the transmitted intensity at the output of the optical fiber decreases (shows a dip) as shown in Fig. 1(b). The resonance condition occurs when the evanescent wave, generated from the reflection of the guided light at the fiber core Au interface, matches with the wavevector of the SP. The Pd layer makes the multilayer sensitive to hydrogen. Pd dissociatively splits and absorbs hydrogen. The formation of the Pd hydride changes the complex refractive index, the lattice constant (and the conductivity) of the Pd.

The sensor response is simulated by combining the theory of local plane waves and a geometric optics approach. The simulation has been performed as described in [23], and the optical constants are taken from [24, 25]. The expansion of the Pd is neglected in our simulations. As shown in Fig. 1(b), the SPR dip shifts upon the hydrogenation of the Pd layer. In fact, in the presence of hydrogen, the change of the Pd refractive index modifies the effective index of the multilayer (since the power flow in the layers is redistributed), which results in modifying the resonance condition. According to our simulation, the SPR shifts to higher wavelengths, while the minimum value decreases because the Pd hydride phase is less absorbing. By measuring these changes, we are able to determine the hydrogen partial pressure. The multilayer design allows us to match the propagative constant between the guided modes and the SP. First, a first metal layer is used to support the SP, i.e. the main collective oscillations of free charge occurs at its interface. Note that this layer makes the sensor insensitive to the Transversal Electric (TE) polarization since the SP is only coupled by Transversal Magnetic (TM) polarized light. Nevertheless, the guided mode cannot be coupled to the SP since the resonance condition is not satisfied. As seen in Fig. 2(a) (black curve), the angular position of the SPR peak for the Au Air system is far beyond the NA of the fiber. We deposit a SiO_2 layer to position the angular resonance peak in the angular range of the optical fiber. With increasing the thickness of the SiO_2 layer, the angular position of the SPR peak shifts to larger angles (i.e. the wavevector of the SP increases) [26]. Consequently, the resonant wavelength shifts towards longer wavelengths when increasing the thickness of the second layer. Finally, the Pd layer is used only as a hydrogen sensitive layer to change the effective index of the multilayer: the intermediate layer is thick enough to almost decouple the SP (and thin enough to avoid multimodes in the metal insulator waveguide).

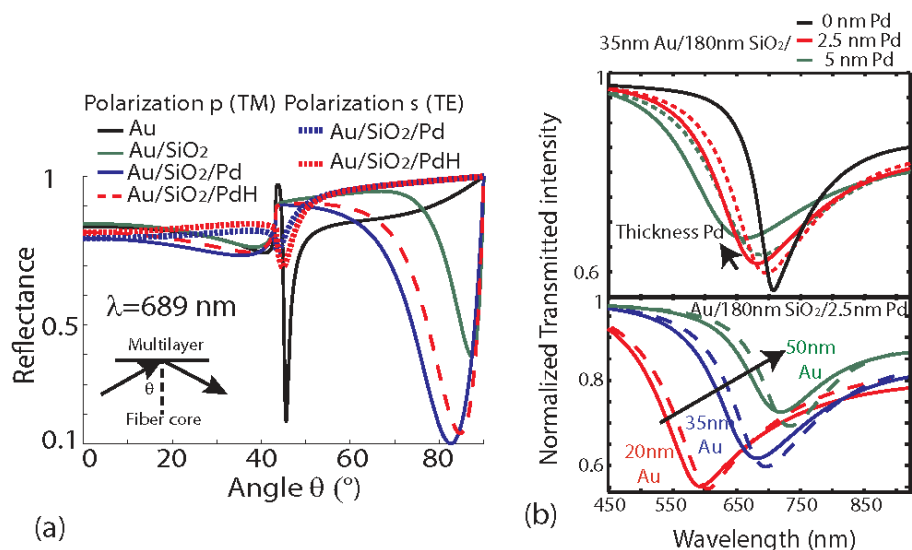


Fig. 2. (a) Schematic representation of the role of each layer. The multilayer stack is deposited on the core of an optical fiber. Each curve shows the reflectance of the corresponding layer as a function of the incident angle. In an optical fiber the light propagates only for high angles (depending on the fiber NA). (b) The transmitted spectrum at the output of the fiber for various thickness. (The coupling is maximal when the intensity drops at 0.5 since only the TM polarized light is coupled to Surface Plasmon).

The thickness of each layer defines the SPR dip (i.e. the propagation length of the SP). Though a thicker Pd layer will enhance the hydrogen sensitivity of the sensor, the Pd layer has to be thin enough in order to avoid suppressing the SPR dip due to the highly absorbing character of Pd. Figure 2(b) shows that increasing the Pd layer tends to widen and decrease the depth of the SPR dip. Moreover, we chose to deposit a very thin Pd film, in order to obtain a fast response. A thickness of 180 nm is chosen for the SiO₂ layer to position the resonance in the middle of the spectrum of the light source -around 700 nm- in order to obtain the best Signal Noise Ratio. A thickness of 35 nm for the Au layer appears to be a good trade-off between the resolution (narrow peak) and the sensitivity of the sensor (shift of the SPR peak), as shown in Fig. 2(b). The role of the thickness is the same as described in details in [23], although the Ag layer was replaced here by an Au layer for experimental reasons. Finally, the Pd thickness is the critical parameter regarding the hydrogen sensitivity, the response time and the reproducibility. To study the importance of the Pd thickness effect, we varied the Pd thickness between 0 and 5 nm.

3. Experimental details

The deposition of the multilayer on a Newport multimode step-index fiber (200 μ m core/ 230 μ m cladding, NA = 0.37) core is done in a multisource AJA magnetron sputtering system. We chose a multimode fiber to realize a simple, "low-cost" and robust sensor (large core diameter). The optical fiber core is made of pure silica, a harder polymer for the cladding and a Tefzel jacket. The optical cladding is thermally removed over a length of 50 mm (+/- 20 mm) after removing the jacket by a mechanical stripping. The optical fiber is then cleaned successively in a methylchloride and acetone ultrasonic bath. The optical fiber is set horizontally in the chamber above the deposition sources. The rotation of the fiber ensures a uniform layer thickness. At a background pressure of 10^{-7} mbar an Ar sputter pressure of 3 μ bar was applied. Au, SiO₂ and Pd were sputtered at an average rate of 1.4 $\text{\AA}/\text{s}$, 0.234 $\text{\AA}/\text{s}$ and 1.5 $\text{\AA}/\text{s}$ respectively. The deposition rates are determined by measuring the thickness of the deposited film on a glass substrate. To obtain the SiO₂ layer, a pure Si target is sputtered using oxygen as a reactive gas. To measure the response of the SPR sensor, a tungsten halogen light

source and an Ocean Optics HR 4000 spectrometer (with a resolution of 0.1 nm) are used. The optical fiber based hydrogen detector is connected via 905 SMA connectors to the light source and the detector. The numerical aperture of the source is larger than that of the optical fiber in order to excite all the fiber modes. However, the measurement is limited by the NA of the spectrometer, which is 0.22.

We measure the total transmitted intensity at the output of the fiber in the spectral range between 500 and 800 nm. Figure 3(a) shows the normalized spectral response of various configurations, which is defined as the measured spectrum divided by the spectrum of the bare optical fiber. As predicted, the resonant wavelength is tunable and depends strongly on the SiO₂ layer thickness. The resonant wavelength is near 640 nm and 680 nm respectively for a 140 nm and 180 nm thick SiO₂ layer as shown in Fig. 3(a) and 3(b), which is in good agreement with the simulated response as shown in Fig. 1(b). The discrepancy of 0.5 to 5% between the measured and simulated value of the resonant wavelength, is most likely caused by a small uncertainty in the deposited thickness (i.e. a variation in the length of the sensing area due to manual fabrication, results in a slight difference in the distance between the sensing area and the targets, and thus a change in deposited thickness).

To investigate the sensor response, we studied the relative change in the transmitted response for each individual sensor. In fact, we cannot directly compare the width and the minimum value of the SPR resonance peak experimentally obtained with our simulations, since the losses may also come from the coupling (source/detector-fiber connection) and the sensing interface (cladding-core interface). Nevertheless, the relative change of the SPR peak in presence of hydrogen is the same between the different samples and insensitive to the intensity fluctuation.

The optical fiber is measured in a gas cell (27 mm x 27 mm x 13 mm). The measurements were carried out at hydrogen concentrations ranging between 0.5% –4% H₂ in Ar at atmospheric pressure and room temperature. The flow rates of each gas were individually controlled with mass flow controllers. The total flow is kept at 250 ml/min. Before the measurements, the gas loading cell is purged several minutes with Ar in order to minimize impurities in the gas system.

4. Hydrogen response and discussion

Adding H₂ to the Ar we observe that the SPR dip changes in all layer geometries as shown in Fig. 3(a). As expected, the SPR dip shifts and the depth of the SPR dip increases. However, the SPR dip shifts toward *shorter* wavelengths, in contrast to our simulation performed shown in Fig. 1(b).

In order to study the response and the reproducibility of the sensor, we consider the Au (35 nm)/ SiO₂ (180 nm)/ Pd (2.5 nm) layer stack. The detection is done either by measuring (i) the amplitude change for different wavelengths or (ii) the resonant wavelength change, as plotted in Fig. 3(b). For the latter approach, a curve fitting Matlab procedure (with Fourier series, 5th order) is used to minimize the random noise. The minimum of the SPR peak is determined from the zero of the derivative function fitted.

The resonant wavelength shifts by 3 nm at 2% H₂ in Ar, while the relative change in intensity depends on the wavelength chosen. The intensity decreases for wavelengths *shorter* and increases for wavelengths longer than the resonant wavelength. In both cases, the optical response of the sensor is reproducible over all hydrogenation cycles but the first cycle shows a non negligible drift. It has been shown that the first hydrogenation cycle causes a relaxation of the build-in stress as a result from deposition [27, 28]. In addition, the first hydrogenation cycle may remove any adsorbed gas species gathered at the surface during transport.

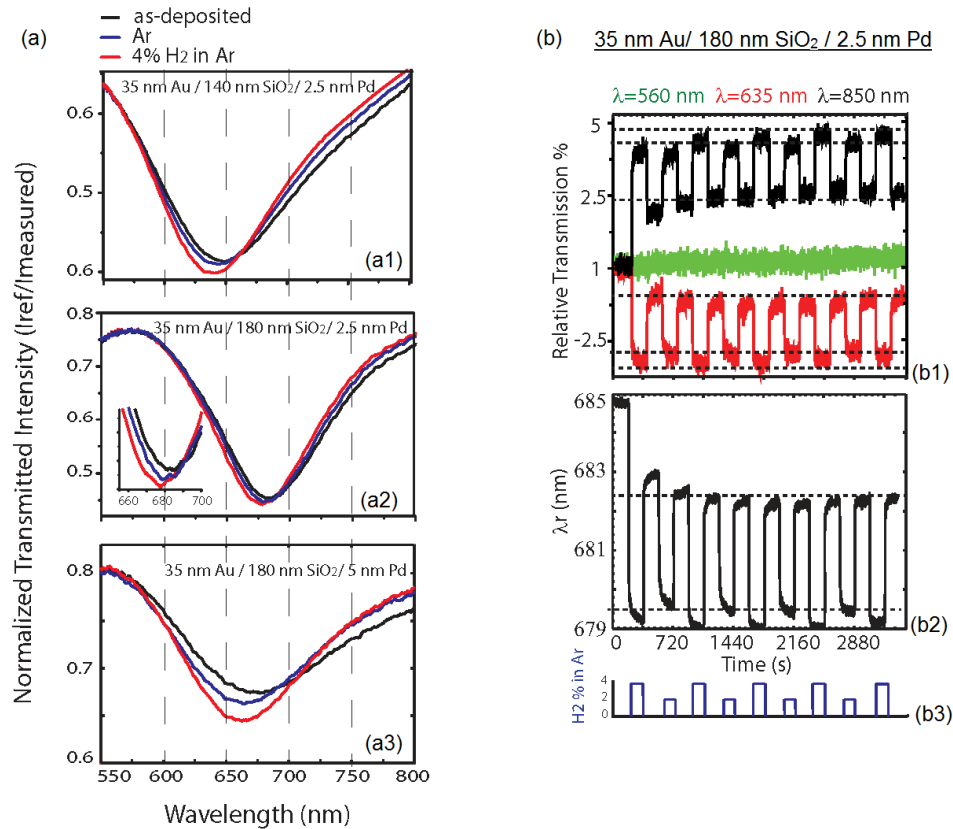


Fig. 3. (a) Normalized transmitted spectrum for a (a1) Au/ SiO₂ (140 nm)/ Pd (2.5 nm), for a (a2) Au/ SiO₂ (180 nm)/ Pd (2.5 nm) and for a (a3) Au/ SiO₂ (180 nm)/ Pd (5 nm) layer stack. The SPR peak shifts in the presence of H₂. (b) The sensor response of a Au (35 nm)/SiO₂ (180 nm)/Pd (2.5 nm) layer stack on successive hydrogenation cycles (at 4% and 2% H₂ in Ar). (b1) The transmitted intensity changes as a function of [H₂] and depends on the selected wavelength. (b2) The resonant wavelength shifts as a function of H₂. (b3) Hydrogen cycles over times.

As shown in Fig. 3(b), the change of the optical signal, amplitude and resonant wavelength is a function of the hydrogen concentration. In particular, the sensor response is related to hydrogen solubility in the metal. Below the critical temperature, the metal hydride exists in two phases called α and β [29]. The α phase characterizes a low solubility (the H atoms occupy randomly the interstitial sites of the metal host lattice). The β phase characterizes a high solubility with 60-70% of all the sites being occupied). During the phase transition (where both phases coexist at the so-called plateau pressure) the number of H atoms increases significantly, which induces a Pd lattice expansion due to the H-H interactions. This 2-phase character is reflected in the behavior of the sensor as depicted in Fig. 4(a). Below the pressure plateau, small changes are observed corresponding to the α phase which limit the minimal detection to 0.5% H₂ in Ar. The observed phase transition, around 1.5 to 2% H₂ in Ar (15-20 mbar), is in agreement with the literature values [30]. The observed sloped plateau is characteristic for an ultrathin Pd film. Above 3% H₂ the sensor response saturates corresponding to the formation of the β phase.

As with all Pd based sensors, a large signal is obtained when applying hydrogen concentrations well above the plateau pressure. In our case, the detection based on wavelength modulation is reliable even for small changes in the hydrogen concentration, well below the plateau pressure. In the case of amplitude sensors small changes in intensity could simply be the result of noise (from the fluctuation of the light source or the presence of bending) instead

of hydrogen. Note, that in our geometry a reliable detection based on amplitude modulation can be done by measuring at several wavelengths having an opposite effect (Fig. 3(b)).

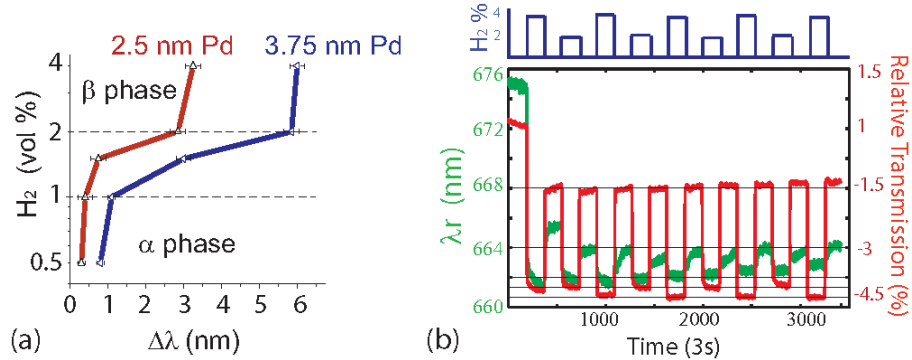


Fig. 4. Au (35 nm)/SiO₂ (180 nm)/Pd sensor dynamical range at room temperature and ambient pressure for different Pd thicknesses. (b) Response of a Au (35 nm)/SiO₂ (180 nm)/Pd (5 nm) layer stack on successive hydrogenation cycles (at 4% and 2% H₂ in Ar), showing the shift of the resonant wavelength and the intensity variation of the minimal value.

The response of our sensor design is fast. Defining the hydriding and dehydriding time as the time it takes to reach 90% of the rise and fall time, we find hydriding times of approximately 3 s at 4% H₂ in Ar with a dehydriding time of about 10 s, as shown in Fig. 5(a). Note that in our experimental setup, the gas mixture reaches the sensor surface after 6-7 seconds. The hydriding time is slightly longer at lower hydrogen concentrations (α phase), as shown in Fig. 5(b), but increases significantly for concentrations close to the phase transition, about 17 s at 2% H₂ in Ar. The plastic deformation occurring during the phase transition could be responsible for this phenomenon [31, 32].

For thin Pd films, the response time is limited by surface processes since the hydrogen diffusion through the Pd layer is negligible [33]. We assume that the improvement of the response time (in comparison with wavelength fiber sensors based on a Pd films thicker than 30 nm) is due to the presence of a discontinuous Pd surface. At room temperature the deposition of Pd causes an island growth mode and for Pd films thinner than 5 nm. It is reported that such a film is made up of a discontinuous network of interconnected islands [34, 35]. The increase of the surface area improves the hydrogen adsorption which may explain our fast response, in analogy to discontinuous film for electrical hydrogen sensor [36]. Furthermore, this assumption could explain the anomalous direction of the SPR peak shift. In our simulation, we have used the dielectric permittivity of the Pd/ Pd hydride obtained for a continuous thin film [23]. The Pd island structure may have an inverse effect on the effective index of refraction of the layer stack upon hydrogenation [37]. In fact, while the change of the refractive index considered in our simulation is responsible for a shift to higher wavelengths, the expansion of the Pd upon hydrogen absorption could explain the opposite direction of the experimentally observed shift.

In comparison with current wavelength fiber sensors (generally based on gratings [3, 5–8]), the response obtained is one order faster. The sensor proposed also shows a better reproducibility. Because of the large core diameter of multimode and the small sensing section (uncladding section inferior to 1 cm), the sensor shows a good robustness and can be developed for industrious systems. In addition, the use of the optical fiber offers the possibility of a flexible, a remote and a multi-point sensor, which can be easily embedded in industrial system. Finally, the design proposed is simple, as compared to plasmonic single point hydrogen sensors such as Pd Localized SPR [17, 18], Nanoantenna [19] and nanostructured Pd film [38] are complex optical devices: they generally need optical systems to illuminate and collect the light from the transducer such as lenses, polarizer and microscope objective.

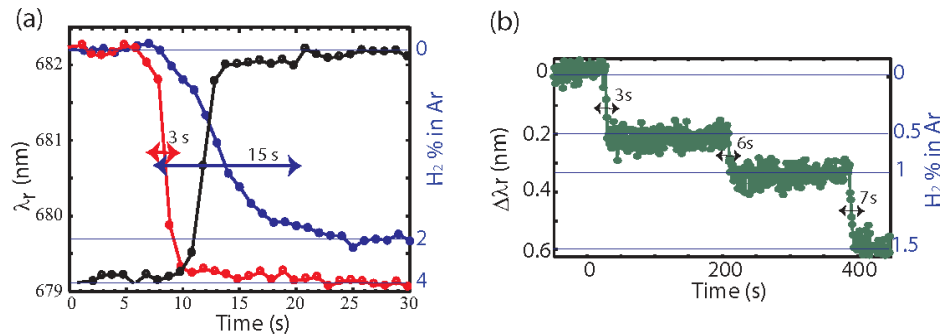


Fig. 5. Response time of a (35 nm)/SiO₂(180 nm)/Pd sensor at room temperature and ambient pressure. (a) Hydriding time at 2% H₂ in Ar (blue line), 4% H₂ in Ar (red line) and dehydriding time (black line). (b) Sensor response at 0.5, 1 and 1.5% H₂.

In order to further optimize the sensor response, we varied the thickness of the Pd film between 0 and 5 nm. As simulated in Fig. 2(b), the shift of the resonant wavelength is larger with an increasing of the Pd thickness as experimentally observed in Fig. 4(a). We observe also that the SPR dip is attenuated: the depth decreases, and the dip is broader for thicker films, as shown in Fig. 3(a), since Pd is a highly absorbing material. In addition, we experimentally found that the resonant wavelength modulation becomes less reproducible for Pd films which are thicker than 5 nm. Though the intensity variation of the SPR minimum is reproducible, the shift of the SPR dip is deteriorated over hydrogen cycles, as shown in Fig. 4(b), for a 5 nm Pd thick. In this case, we think that the film becomes more and more continuous over hydrogen cycles due to the Pd expansion (the Pd islands aggregate during the hydrogen cycling). The competitive effect of the expansion and the change of the Pd refractive index upon hydrogenation on the shift of the SPR dip could explain the decrease of sensitivity over hydrogen cycles. Further investigations have to be done to address this point. Finally, we experimentally conclude that the Pd layer has an optimal thickness of about 3.75 nm.

7. Conclusion

In conclusion, we experimentally demonstrated for the first time a fast optical fiber SPR hydrogen sensor based on wavelength modulation. We significantly decrease the response time to only a few seconds by optimizing the Pd thickness. In contrast to sensors sensitive to intensity fluctuation, a threshold could be used in the post-processing to meet the response time required for applications. The proposed design is simple, stable and takes advantage of optical fiber properties, such as remote sensing. The sensor response shows a very good reproducibility with a satisfying dynamic range, most probably due to the used Pd thickness since the plasmonic multilayer permits the use of an ultra thin Pd film. Our results show that using the SPR is a promising approach for hydrogen sensing in order to obtain a fast response based on wavelength modulation. In this framework, new multilayer designs could be developed in order to realize reliable fiber sensors. Since the Pd layer is simply used to change the surrounding index medium, any other sensitive material such as Pd alloys [32] or embedded metal nanoparticles/discontinuous films in a protective polymer film, or protective layers can be added in the proposed design in order to decrease the cross-sensitivity and increase the lifetime of the sensor.

Acknowledgment

The authors thank Lennard Mooij and Ali Dabirian for useful discussions and comments. This work was financially supported from the Region Alsace in France and the Nederlandse Organisatie voor Wetenschappelijk Onderzoek NWO through the Sustainable Hydrogen Programme of Advanced Chemical Technologies for Sustainability program.